Intraparticle Diffusion Mechanisms in SC Sunflower Oil Hydrogenation on Pd

E. Ramírez, M. A. Larrayoz, and F. Recasens
Dept. of Chemical Engineering, ETS Enginyeria Industrial de Barcelona, Universitat Politècnica de Catalunya, E-08028 Barcelona, Spain

DOI 10.1002/aic.10753
Published online December 21, 2005 in Wiley InterScience (www.interscience.wiley.com).

In this work, intrinsic kinetics were decoupled from reactant diffusivities in the SC sunflower oil hydrogenation reaction on Pd/C using a steady-state diffusion and chemical reaction model under isothermal conditions in order to obtain low trans and stearic final products. A numerical solution combined with nonlinear parameter fitting was employed to solve this model. First, runs with small size of catalyst (0.4 mm) allowed to obtain kinetic constants irrespective of the diffusivity settings. Then, in a second set of runs, reactions were repeated on larger sizes of catalyst (up to 1 mm), that is, in the diffusion-limited regime. The results show that while hydrogen is transported by bulk pore diffusion, the oil seem to diffuse by surface diffusion. Diffusivity of H_2 is about 10 times that of triglycerides. The overall diffusivity for triglycerides is about 10^{-8} m^2/s, and changes 3 times with an increase in pressure, and 20 times with an increase in T. Linoleate selectivity (S_{LO}) and specific isomerization (S_i) also improve with decreasing the diffusion path. © 2005 American Institute of Chemical Engineers *AIChE J,* 52: 1539–1553, 2006
Keywords: vegetable oil hydrogenation, supercritical propane, trans content, kinetics, intraparticle diffusion, palladium catalyst

Introduction

Supercritical fluid (SCF) technology is becoming important in the lipid and food industries for a variety of applications. So far, however, the emphasis has been on extraction processes[1] and on some heat and mass transfer operations, thus not involving chemical transformation. Reaction and catalytic applications in SCF clearly lag behind (see, for example, Brunner[2]) except for certain industrial polymerizations,[3] where a potential is shown to exist, although in principle these are not related to biotechnology or biomolecules. In an early review, however, Subramaniam and McHugh[4] indicate the interest of catalysis in SCF. The benefits of SCF in catalysis have been emphasized in certain model isomerization reactions for controlling coke deposition[5] and improving intraparticle diffusion.[6]

The purpose of vegetable oil hydrogenation in general is to obtain a more stable product (no oxidation on storage), together with a suitable texture and melting-temperature range at mouth conditions for human use as margarine and shortenings. A catalytic slurry process is customary in the vegetable oil hydrogenation industry, with nickel (Raney or supported) or supported palladium as catalysts, an otherwise well-established technology with well-known catalyst types.[7-10] The low solubility of hydrogen in oil under conventional operating conditions, together with the transport resistances, leads to very low reaction rates. According to the half-hydrogen theory,[11] the formation of *trans* fatty acid increases when the hydrogen concentration at the catalyst surface decreases.

Fatty acid triglycerides exhibit *cis–trans* isomeric forms: when fatty compounds are unsaturated, it is usually the naturally occurring *cis*-isomer; the *trans*-isomer appears only during hydrogenation. If uncorrected, the *trans* content can be as large as 40 wt % as in the conventional, low-pressure, slurry reactor process.[10] Although the effects on human health of *trans*-isomers are not clear, they are suspected to act as precursors for the undesirable cholesterol type so likely to affect

Correspondence concerning this article should be addressed to M. A. Larrayoz at m.angeles.larrayoz@upc.edu.

Table 1. Tortuosity Factors for High-Pressure Extraction of Porous Solids*

Author(s)	Operating Conditions	Solid Matrix	Tortuosity Factor, τ
Knaff-Schlünder[57]	308–328 K 12–22.6 MPa	Bronze, $\varepsilon_p = 0.3$ Pores 8–20 μm	τ indep. of d_p and P, $\tau = 0.4$–0.54
Recasens et al.[58]	Desorption EtAc 300–338 K $P < 13$ MPa	Regeneration Activated carbon (micro-, macroporous)	Linear driving force model $\tau = 4$
Madras et al.[73]	Naphthalene adsorption, 298–318 K 8–31 MPa	Micro- and macroporous alumina	τ const. w/P and T, $\tau = 3.29$ (av)
Lai and Tan[36]	Toluene adsorption	Micro- and macroporous activated carbon, $\varepsilon_p = 0.45$	τ depends on pressure, $\tau \sim 0.2$–0.6
Stüber et al.[23]	DiCl–benzene extraction from sintered bronze	Bronze, macropores $\varepsilon_p = 0.20$ to 0.25 pore size ~ 15 μm	τ const. w/P but varies w/T, $\tau \sim 0.22$ to 0.62
Lee and Holder[56]	Adsorption of toluene and naphthalene	Silica gel (micro- and macropores)	$\tau = 3.49$ (av)

*Refer to Stüber et al.[23]

cardiovascular health. To date, Denmark is the only country in the world where the Ministry of Health since May 2003 has limited by law the *trans* content to <2 wt % on fatty acid components for human ingestion. The committee of experts Codex Alimentarius of the Food and Agriculture Organization of the United Nations continues to debate regarding the inclusion of *trans* fatty acids content on food labels. On the other hand, the European Union (EU) is favorable to include this on the label, but legal action is yet to be taken. In the United States, the government [through the Food and Drug Administration (FDA)] has put forward a campaign (announced by the Surgeon General in 2003) to label by law the *trans* content and (or together with) the saturated fat content, before 2006. The efforts of King and coworkers[12] to develop a low *trans* process at the FDA are in this direction.

A key factor in the use of supercritical solvent in vegetable oil hydrogenation is that under certain conditions, the concentrations of H_2, triglycerides (TGs), and solvent can be varied independently over the external catalyst surface,[13] without any limitation, provided only that phase separation is avoided. Such a one-phase condition cannot possibly be achieved in the conventional low-pressure slurry process, where the reaction rate and selectivities are determined by the availability of reactant dissolved in the liquid from gas bubbles, and its transport through the liquid and through the liquid–solid boundary layer onto the catalyst. The resulting catalytic reaction rates, in high-pressure systems and low-pressure processes, have been critically reviewed.[14]

Most of the commercial SCF hydrogenations have been filed by Härröd and coworkers[15] and Degussa scientists in the EU[16,17] and elsewhere. In the United States, the work of King and coworkers,[12] at the Department of Agriculture, is very important in this regard because it opens the possibility of a new process in lipid chemistry.

In a previous work, we used the design of experiments and response surface methodology[18] to achieve optimum hydrogenation conditions for Pd catalyst in SC propane in a CST reactor. Ramírez et al.[19] showed that it was possible to obtain a hydrogenated fat of about 2–3 wt % *trans* content in a single pass through the reactor in a continuous process, with an iodine value (IV) of about 70 (starting with a value of 130). Triglyceride from sunflower oil was the raw material. Furthermore, kinetics using the Hashimoto et al.[20] scheme provided information on the kinetics for hydrogenation on a commercial-size Pd/C catalyst.

Further work shows[21] that when mass transfer resistances on the catalyst are made small, the amount of the *trans*-C18:1 is minimized; thus the *trans* lower bound can still be lowered. External mass transfer can be made negligible using a high flow velocity over the catalyst bed. Ramírez et al.[19] give the range of linear velocity where such selectivity enhancement occurs. With respect to the internal resistance, the properties of the SCFs should provide rapid intraparticle diffusion rates, thus improving selectivity to the desired intermediate products.

Five possible facts make intraparticle mass transfer distinct from molecular or free diffusion. First, the inner path is tortuous, so the length of the diffusion path from the external surface to the particle center is longer than the particle radius. That extra length over the particle radius length is called the *tortuosity factor* (τ), and should normally be >1, usually $\tau = 3$–10.[22] Second, if the solid material is relatively impermeable, not all the cross-sectional area is available for the transport flux; only a fraction, ε_p, is available. Third, the pore walls can contribute to the transport because they can adsorb and desorb reactant or product, thus modifying their transport rates. This is the so-called *surface diffusion* (or surface migration), whereby the adsorbed concentration driving force causes the flux. Fourth, in very fine pores or for a very low pressure gas, the walls can slow down transport if molecules collide with the walls more often than they do with each other (a phenomenon called *Knudsen diffusion*). Usually, the first three mechanisms are present at high-pressure diffusion in SCF. Knudsen diffusion, however, is unlikely to contribute to diffusion in the case of high-pressure gases. By contrast, surface diffusion can be very important in SCFs, as has been shown in nonreacting (extraction) applications by Stüber et al.[23] as summarized in Table 1.

Another fifth diffusion mode is observed. This is restricted diffusion in very fine pores. This takes place when the dimensions of the solute molecule and the pore are comparable. A number of studies[24-27] have shown that restricted diffusion occurs in silica–alumina and zeolite catalyst with pore diameters of $<5 \times 10^{-6}$ mm. Satterfield et al.[27] obtained experimen-

tal data on such diffusion. The experimental data were correlated by the equation

$$\frac{D_e}{D} = \frac{\varepsilon}{\tau} 10^{-2d_s/d_e} \quad (1)$$

where d_s is the solute critical diameter, defined as the diameter of the smallest cylinder through which the solute molecule can pass without distortion, and d_e is the pore diameter. The ratio of d_s to d_e is known as the hindered diffusion factor. Satterfield et al.[27] considered that this factor is in the range 0.1–0.5.[28]

Additionally, if the porous matrix is a composite of channels and inert or active regularly located islands, different diffusion rates in the two regions may strongly affect the overall diffusion rate.[29] In fact several diffusion models for catalysts have been proposed to account for the flux in two-region media. In this case we have the Wheeler model,[30] the random-pore model,[31] and later developments (the models of Stewart and coworkers[32] and Patel and Butt[33]). Today, low-pressure gas diffusion in a network of pores can be simulated to assess tortuosity factors when the Knudsen mode of diffusion is present.[34]

The overall effective diffusivity D_e can be expressed as a result of the combination of two main effects: (1) a pore volume diffusion with an effective coefficient based on bulk diffusivity and (2) a surface diffusion contribution. The effective diffusivity can be expressed as

$$D_e = \frac{D\varepsilon_p}{\tau} + \frac{\rho_p K_A D_s}{\tau} \quad (2)$$

with both types of diffusion mechanisms applying for two types of reactants, the triglycerides and hydrogen. There are two assumptions in this equation: (1) The tortuosity factor for surface diffusion is the same as that for bulk pore diffusion[35] (note that this should not be so), and (2) it is assumed that surface migration occurs at near adsorption equilibrium, where K_A is the Henry-type equilibrium constant on the solid from the high-pressure fluid. Again, in activated carbon Lai and Tan[36] found that the Toth isotherm rather than the Henry isotherm controlled adsorption. D_s is the common surface diffusion coefficient with an adsorbed concentration driving force. Because these quantities are seldom available, an average or apparent tortuosity factor is used. A change in temperature may largely affect K_A, which may lower the effective diffusivity with increasing temperature, thus showing a reversed-temperature mode. This is true in many reactions at low pressure where adsorption is generally exothermic; thus the negative temperature dependency provides evidence to assess the presence of surface diffusion. Therefore surface diffusion is usually distinguishable pore bulk diffusion in low-pressure catalysis because of an inverse-temperature effect.

This may be different in a supercritical fluid. In this case, the retrograde adsorption can be endothermic within a certain high-pressure range near the critical point or well above it.[37] Therefore in a supercritical fluid, the positive temperature dependency of the diffusivity makes surface diffusion indistinguishable from the normal bulk diffusion. We will find this effect in the experiments.

Discussions on the theoretical aspects of surface diffusion were previously presented.[35,38,39] Values of D_s have been reported by Schneider and Smith.[40] For hydrocarbon gases in the usual catalyst substrate materials, values in the range 10^{-9}–10^{-7} m^2/s are observed for low-pressure gas-phase reactions.

Information from the open literature on the possible role of intraparticle diffusional limitation in oil hydrogenation in slurry reactors at low pressure is very limited.[41] For low-pressure hydrogenation of cottonseed oil, D_e for hydrogen is approximately 70 times as large as $D_{e,TG}$ in cottonseed oil.[42] Intraparticle diffusion limitation of triglycerides has, among others, a pronounced effect on linoleate selectivity (S_{LO}), as can be seen from the decrease of S_{LO} with increasing particle diameter.[43]

Coenen[44] summarized the data on diffusion limitation and reported for a narrow pore catalyst (mean pore diameter $d_{pore} \cong 4 \times 10^{-6}$ mm) a 50% decrease in activity relative to a medium pore ($d_{pore} \cong 6 \times 10^{-6}$ mm) and wide pore ($d_{pore} \cong 8 \times 10^{-6}$ mm) catalyst. Colen et al.[45] observed intraparticle diffusion in trioleate hydrogenation from which they calculated intraparticle triglycerides diffusion coefficient $D_{e,TG} = 2 \times 10^{-11}$ m^2/s (wide pore catalyst) and 4×10^{-12} m^2/s (medium pore catalyst) at 373 K and an absence of hydrogen limitation.

For fatty acid methyl ester hydrogenation over Pd/C catalyst, Tsuto et al.[46] could verify the observed shunt reactions by incorporating intraparticle hydrogen diffusion limitation, although not very accurately because of the insensitivity of the curves for the value of $D_{e,H_2} = 3.6 \times 10^{-9}$ m^2/s at 443 K. An estimated value of $D_{e,H_2} = 4 \times 10^{-9}$ m^2/s at 443 K was obtained from the experimental data by Andersson et al.[47] and Ganguli and Van den Berg,[48] which is in agreement with the data of Tsuto et al.[46]

Jonker et al.[49] investigated the intraparticle diffusion limitation in the hydrogenation and isomerization of fatty acid methyl esters (FAMEs) and soybean edible oil [triacylglycerol (TAG)] in porous nickel catalyst under reactive and inert conditions. They found that FAME hydrogenation reaction at 443 K appears to be controlled by intraparticle diffusion of hydrogen ($D_{e,H_2} = 1.6 \times 10^{-10}$ m^2/s). In the hydrogenation of triglycerides, the triglycerides appear to be diffusion limited ($D_{e,TG} = 3.3 \times 10^{-12}$ m^2/s) rather than H_2, which agrees with the literature. Veldsink[50] proposes the effective triglyceride coefficient equal to the liquid-phase triglyceride diffusion coefficient divided by 10, which is of the order of magnitude of the first term of Eq. 2 with typical values of the factors, ε_p and τ. Thus two features seem evident: first, nothing new on the diffusion mechanism is given; second, the order of magnitude of the bulk pore diffusion values is 10^{-10}–10^{-12} m^2/s for the triglycerides and FAMEs.

The lack of experimental data related to intraparticle diffusion at high pressure is surprising in the light of the substantial effects that intraparticle limitation can have on the selectivity of the reaction. In the case of SCF systems, the situation is not different: there is a dearth of available diffusion data. The knowledge and the ability to predict transport properties in SCFs and the ability to predict them are of considerable importance in the understanding and improvement of process efficiency. Because of the high pressure involved, these systems are highly nonideal and are not readily described by predictive mathematical models. In the numerous reviews of

Table 2. Scope of Reaction Conditions

Solvent	Propane (99.5% Purity)
Feed Composition	
H_2 (mol %)	4
Sunflower oil*	1
Solvent	95
Pressure (MPa)	20 and 27.5
Temperature (K)	456 and 483
Catalyst	2% Pd/C
Catalyst mass in reactor (g)	0.25 and 0.8
Iodine value reduction (%)	30 and 44
Catalyst size (mm)	0.47, 0.92, and 2
Number of runs	8
WHSV (h^{-1})	300 and 900

*Aldrich Chemical (C16:0: 6%; C18:0: 7%; C18:1: 19%; C18:2: 68% in wt % as FAME.

SCFs, specific mention is made of the lack of experimental diffusion data.

Liong et al.[51] developed a simple experimental method that has been used to determine diffusion coefficients in several SCF systems mainly in supercritical carbon dioxide (SC CO_2). Diffusion and thermodynamic measurements by SFC are reviewed by both Roth[52] and Suárez et al.[53] Van den Hark[54] made a rough estimate of the effective FAME diffusivity in SC propane based on measured diffusivities in SC CO_2[55] in the order of 10^{-9} m^2/s at 553 K and 15 MPa. For hydrogen in SC propane, diffusivity was considered in the range of 10^{-7} m^2/s from the estimation proposed by Satterfield[22] at low pressure.

For the case of nonreacting SCF systems, Stüber et al.[23] summarized the available data (see Table 1). These data should be judged in light of Eq. 2, that is, with surface diffusion playing a central role. Lee and Holder[56] saw no influence of pressure or temperature on τ (always $=3$–4). By contrast, Lai and Tan[36] indicate a strong influence of pressure and a minor influence of temperature, and their values show for the first time that D_e/D is $\gg 1$ in SC CO_2 (sometimes two- or threefold), which is a striking feature (implying $\tau < 1$). This was on a micropore network. Knaff and Schlünder[57] found a similar feature but on sintered bronze macroporous rods from which naphthalene or caffeine is extracted. The data reported by Lai and Tan[36] fall on the same low tortuosity factors. In Table 1 it seems that when τ is an adjustable parameter, and the adsorption takes place on active sites, it behaves abnormally. In some cases (Recasens et al.[58]) a previous tortuosity factor was fitted together with other adsorption parameters, whereby minimizing two parameters could lead to some error. In the work of Stüber et al.[23] who found $\tau \sim 0.2$–0.6 in a macropore matrix, results were also quite abnormal (see the last row of Table 1). In any case, in the present work we have devoted a greater degree of care to the methods for estimating the molecular diffusivities of Eq. 2, so the factor D_e/D is not likely to be affected by uncertainties in D arising from T or P. These methods are the estimation procedures reported by Sun and Chen[59] and Catchpole and King,[60] today considered most reliable.

The aim of this study was to measure the intraparticle diffusivities of the triglycerides and hydrogen under catalytic hydrogenation reaction conditions using propane as a supercritical solvent, for 2% Pd on activated carbon (a microporous matrix). Our object was to gain further insight into the mass transport mechanisms in SC fluids within the pores of the catalyst. Because the reacting fluid is quite dilute in reactants (1 mol % oil), diffusivities were taken to be the infinite dilution values in the fluid.

Experimental

The experimental conditions and the catalyst, particle sizes, and solvents used, together with the ranges of pressure and temperature, are shown in Table 2. The details of the reactor, feed system, and high-pressure H_2 system were given in previous publications and will receive no further comment herein.[19] We only mention here that a radial-flow, internal recycle, mixed-flow catalytic reactor was used, so there was the possibility of carrying out reactions under the absence of external temperature and concentration gradients.

Chemical analysis of FAMEs in the feed and in the hydrogenated product was performed with silver ion (Varian, Madrid, Spain) column by liquid chromatography on a Waters HPLC apparatus. The methyl esters obtained by transesterification (method of Wijs) were injected in the chromatograph. The elution solvent was acetonitrile. Iodine values of the feed sunflower oil and on the hydrogenated product were done using the Wijs procedure. The analytical methods were previously described in detail by Ramírez et al.[19]

Strategy

For simple first-order catalytic reactions, the particle Thiele modulus (function of k and D_e) is decoupled using two catalyst sizes in such a way that both the kinetic constant and the diffusivity affect the rate. If a powdered form of catalyst particle is available, intrinsic kinetics can be evaluated directly on this small size (thus with an effectiveness factor $\cong 1.0$) and using the larger particle size to infer the diffusive properties of the reactant.[61] We have used that strategy herein, except that a more complex reaction network is present so the multispecies system should be considered (refer to the reactions of Figure 1). These are known to be irreversible, first order in triglyceride and half order in hydrogen, except for the last two reactions, which give stearates that are first order in hydrogen.

Our strategy was as follows. The true intrinsic hydrogenation kinetics from several experiments in the absence of diffusion limitation was determined from small particle diameters. Then, the diffusion coefficients were determined from reaction experiments under diffusion-limited conditions. The best fits of the steady-state diffusion and chemical reaction with the previously available kinetic constants to experiments carried out

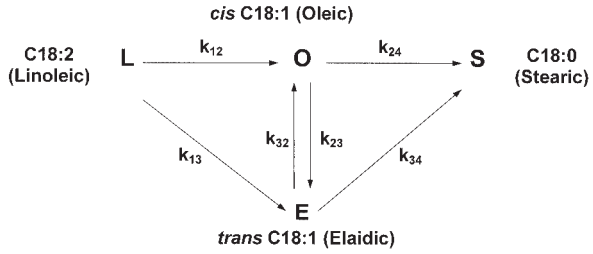

Figure 1. Interconversion of glycerol esters upon hydrogenation; see Table 2 for the raw sunflower oil composition.

Table 3. Effect of Particle Diameter on Hydrogenation of Sunflower Oil in SC Propane*

Reaction Run	Temperature (K)	Particle Size** (mm)	Conversion (%)	Global H_2 Reaction Rate (mol s^{-1} kg $cat^{-1} \times 10^4$)
1	456	0.92	30.6	1.23
2	456	0.47	36.8	2.16
3	484	0.92	36.5	2.26
4	484	0.47	43.6	3.48

*Experimental conditions: 2.5×10^{-4} kg of 2% Pd/C at 20 MPa, feed composition (oil:H_2:propane) 1:4:95 mol %. $W/F = 4.2$ s.
**Crushed and sieved.

under diffusion-limited conditions yielded the diffusivities. The rate equations are used to investigate the effects of intraparticle hydrogen and triglyceride diffusion on the hydrogenation rate. Finally, the ratios of the effective diffusivity to the molecular diffusivity, estimated by means of correlations, were determined under several operating conditions for triglycerides as well as hydrogen to establish which type of diffusivity predominates within the porous catalyst particle. In this way a limited number of reaction runs is required (Table 2).

Internal mass transport resistance

For the above strategy it is necessary that internal mass transport affects the reaction rate, so the catalyst diameter was changed in preliminary runs (see Table 3). As seen, for constant temperature the rate of reaction is reduced on the larger particles. The results in Table 3 thus indicate that internal transport limitation exists at these low concentrations using large catalyst particles. If we consider the 0.47- and 0.92-mm particles (Table 3), the hydrogenation rates on these particles at the same temperatures are not exactly inversely proportional to the particle sizes, so strong intraparticle resistance in these particles is not present. This suggests that the hydrogenation on the smallest particles (0.47 mm) can be closer to 90–100% catalyst effectiveness ($\eta \cong 1$) rather than to the asymptote $\eta = 1/\phi$ on the η–ϕ plot. The actual approach of the 0.47-mm particles to the 100% effectiveness can be judged using the Weisz–Prater modulus using power-law kinetics.[62] The application of the observable modulus to these particles gives a very small value of the modulus, indicating that reaction is not affected by pore diffusion. In this calculation the true reaction order of H_2 has to be used. Ramírez et al.[19] found it to be half order, so in the calculations we used 1/2 or first order with respect to H_2, given that there can be an assured uncertainty. In both cases the modulus is very small. The advantage of the Weisz–Prater modulus is that it requires measured rates, such as those of Table 3, and not kinetic constants as in the case of the Thiele modulus.

In summary, the chemical kinetics can then be determined from the smallest particle diameter where the intraparticle resistance is considered to be small. Based on the values obtained, the effective diffusivities of oil and H_2 were obtained for the largest catalyst particle (see Table 4). The sensitivity of the proposed model with the H_2 and the oil effective diffusivity values was proved for several particle diameters. Finally, the linoleate selectivity (S_{LO}) along with the specific isomerization (S_i), defined in terms of the overall diffusion fluxes (based on the fitted concentration profiles within the catalyst pellet), were determined.

Diffusion and reaction in catalyst particles

A slab of thickness L will be considered, with the origin of coordinates at the midplane ($x = 0$). The hydrogenation is catalyzed within the porous matrix with an intrinsic rate of reaction expressed in mol kg cat^{-1} s^{-1}. The following assumptions will be made: (1) the mass-transport process is in one direction through the porous structure and may be represented by a Fickian expression; (2) there is no net convective transport contribution; (3) there is no fluid-to-particle mass-transfer resistance external to the slab; and (4) the medium is isotropic. For this case, the steady-state mass balances of the chemical species inside, an elemental volume of slab of thickness dx, gives

$$D_{e,TG}\frac{d^2C_i}{dx^2} + r_i\rho_p = 0 \qquad i = \text{L, O, E, S} \tag{3}$$

$$D_{e,H_2}\frac{d^2C_{H_2}}{dx^2} + r_{H_2}\rho_p = 0 \tag{4}$$

Here $D_{e,TG}$ and D_{e,H_2} are, respectively, the effective diffusion coefficients for oil and hydrogen in the reaction medium; and C_i and C_{H_2} are the concentrations of the reactants, respectively. In this case, the effective diffusivities for the components of the oil were assumed to be the same because the components are of similar structure and molecular weight.[63]

The zero flux boundary conditions at the slab center plane are given by

$$\frac{dC_i}{dx} = \frac{dC_{H_2}}{dx} = 0 \qquad \text{at} \qquad x = 0 \tag{5}$$

At the particle surfaces ($x = \pm L/2$) no external mass transfer resistance is considered, and thus

$$C_i\big|_{L/2} = C_{i_s} \qquad i = \text{L, O, E, S, } H_2 \tag{6}$$

The kinetic expressions for the intrinsic rates of formation for each component obey the previously published hydrogenation scheme[20] that gives rise to the following set of kinetic expressions:

$$r_L = -(k_{12} + k_{13})C_L\sqrt{C_{H_2}} \tag{7a}$$

$$r_O = k_{12}C_L\sqrt{C_{H_2}} - k_{23}C_O\sqrt{C_{H_2}} + k_{32}C_E\sqrt{C_{H_2}} - k_{24}C_OC_{H_2} \tag{7b}$$

$$r_E = k_{13}C_L\sqrt{C_{H_2}} + k_{23}C_O\sqrt{C_{H_2}} - k_{32}C_E\sqrt{C_{H_2}} - k_{34}C_OC_{H_2} \tag{7c}$$

$$r_S = k_{24}C_OC_{H_2} + k_{34}C_EC_{H_2} \tag{7d}$$

$$r_{H_2} = -3k_{12}C_L\sqrt{C_{H_2}} - 3k_{13}C_L\sqrt{C_{H_2}} - 3k_{24}C_OC_{H_2} - 3k_{34}C_EC_{H_2} \tag{7e}$$

Table 4. Experimental Reaction Runs on 2% Pd/C for Determination of Intraparticle Diffusion at Constant Final Iodine Value (80–100)*

Reaction Run	Temperature (K)	Pressure (MPa)	Catalyst Particle Size (mm)	Catalyst Mass (kg × 10^4)	Global H_2 Reaction Rate (mol s^{-1} kg^{-1} × 10^4)
5	456	20.0	2	8.0	0.87
6	456	27.5	2	8.0	0.58
7	483	20.0	2	8.0	1.14
8	483	27.5	2	8.0	0.82

*Feed composition (oil:H_2:propane) 1:4:95 mol %.

The above kinetic constants were measured on commercial-size pellets (2% Pd/C, 2 mm in size) so they are not likely to coincide with the intrinsic values. The system of differential equations (see Eqs. 3 to 7) defines a two-point boundary-value problem that is solved numerically using a shooting-type method. This involves converting the second-order ordinary differential equations (ODEs) to coupled pairs of first-order ODEs where z is the new function defined as a diffusion flux as follows:

$$z_i = \frac{dC_i}{dx} \qquad i = \text{L, O, E, S} \tag{8}$$

$$z_{H_2} = \frac{dC_{H_2}}{dx} \tag{9}$$

$$D_{e,TG}\frac{dz_i}{dx} + r_i\rho_p = 0 \qquad i = \text{L, O, E, S} \tag{10}$$

$$D_{e,H_2}\frac{dz_{H_2}}{dx} + r_{H_2}\rho_p = 0 \tag{11}$$

An initial-value problem is created by guessing a concentration value for the species at the center of the catalyst slab ($x = 0$). A set of 10 ODEs results. This is solved using a fourth-order Runge–Kutta method with a small step size. Then, the guessed value of the concentrations at the center is adjusted using the secant method[64] until the value of the concentrations at the external surfaces ($x = \pm L/2$, as computed by the integration) converges to the stated boundary condition. Because a well-mixed reactor without external resistances is used, the fitted concentrations correspond to the known exit concentrations from the CSTR. These are known from the steady-state reaction experiments.

For a given set of kinetic and diffusion parameters, all the above procedures will fit boundary conditions at the external surface. Then the intraparticle concentration profiles for reactants and products can be calculated. Next, it is necessary that the calculated rates over the particle volume should match the observed reaction rates over the particle volume. The overall rates can be determined from the diffusion fluxes at the external surface of the particle. These can be readily evaluated, so that

$$r_{p,i} = \left[\frac{D_{e,i}}{x\rho_p}\left(\frac{dC_i}{dx}\right)\bigg|_{x=L/2}\right] \qquad i = \text{L, O, E, S, H}_2 \tag{12}$$

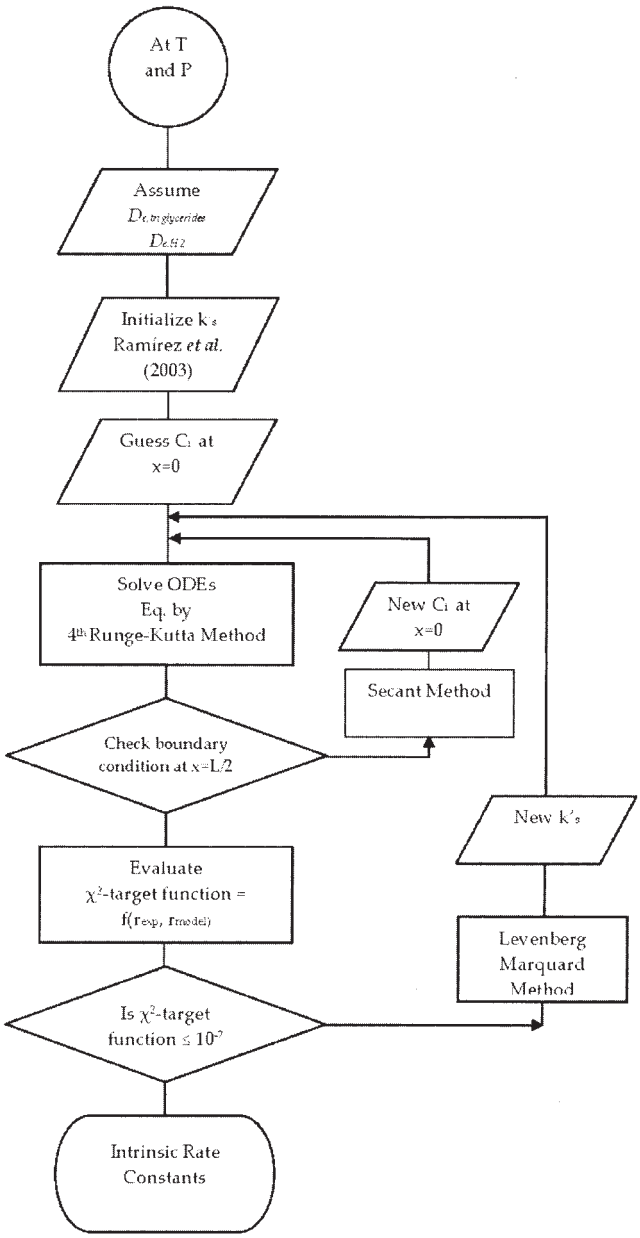

Figure 2. Flowchart for the parameter fitting procedure for the smallest particle diameter catalyst: d_p = 0.47 mm, 2% Pd/C.

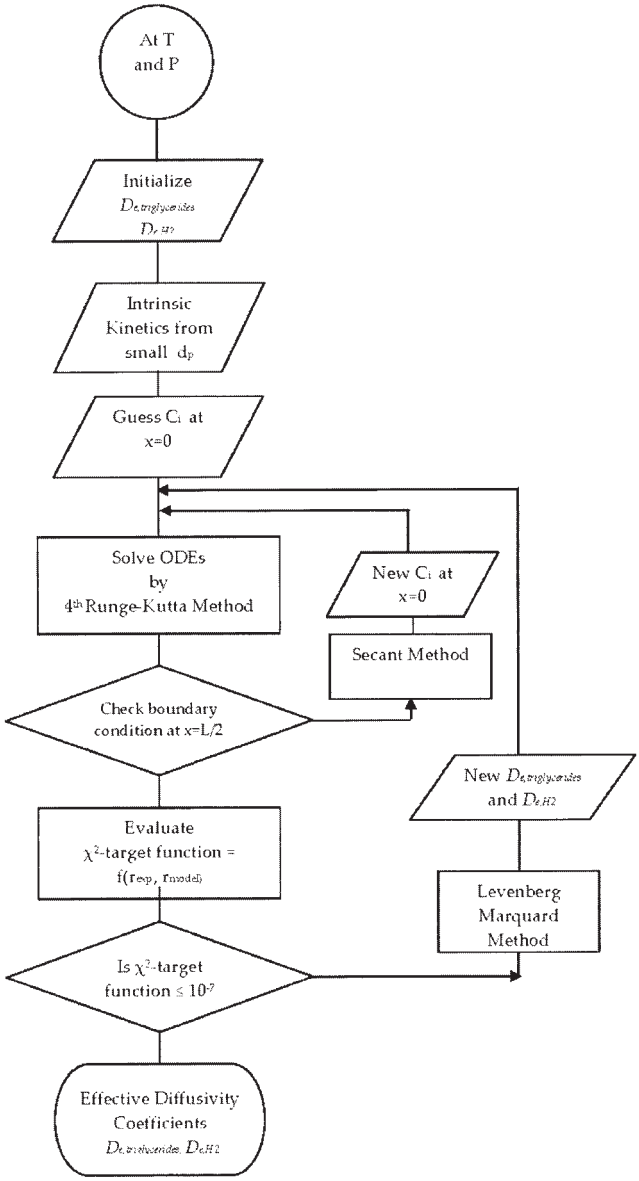

Figure 3. Flowchart for the parameter fitting procedure for the largest particle diameter catalyst: d_p = 2 mm, 2% Pd/C.

where $r_{p,i}$ is the reaction rate per unit mass in the pellet in mol kg^{-1} s^{-1}.

The above differential equations were solved for several estimated values of the effective diffusivities $D_{e,TG}$ and D_{e,H_2} using the intrinsic kinetic rate constants obtained previously. The optimization of these values was achieved by minimization using the Levenberg–Marquardt algorithm. The objective function was defined as the residual sum of squares of the experimentally observed reaction rates and the predicted rates of reaction for the hydrogenation reactants. The optimization was done simultaneously with the numerical integration of the model equations. The double-iteration solution procedure is summarized in Figures 2 and 3.

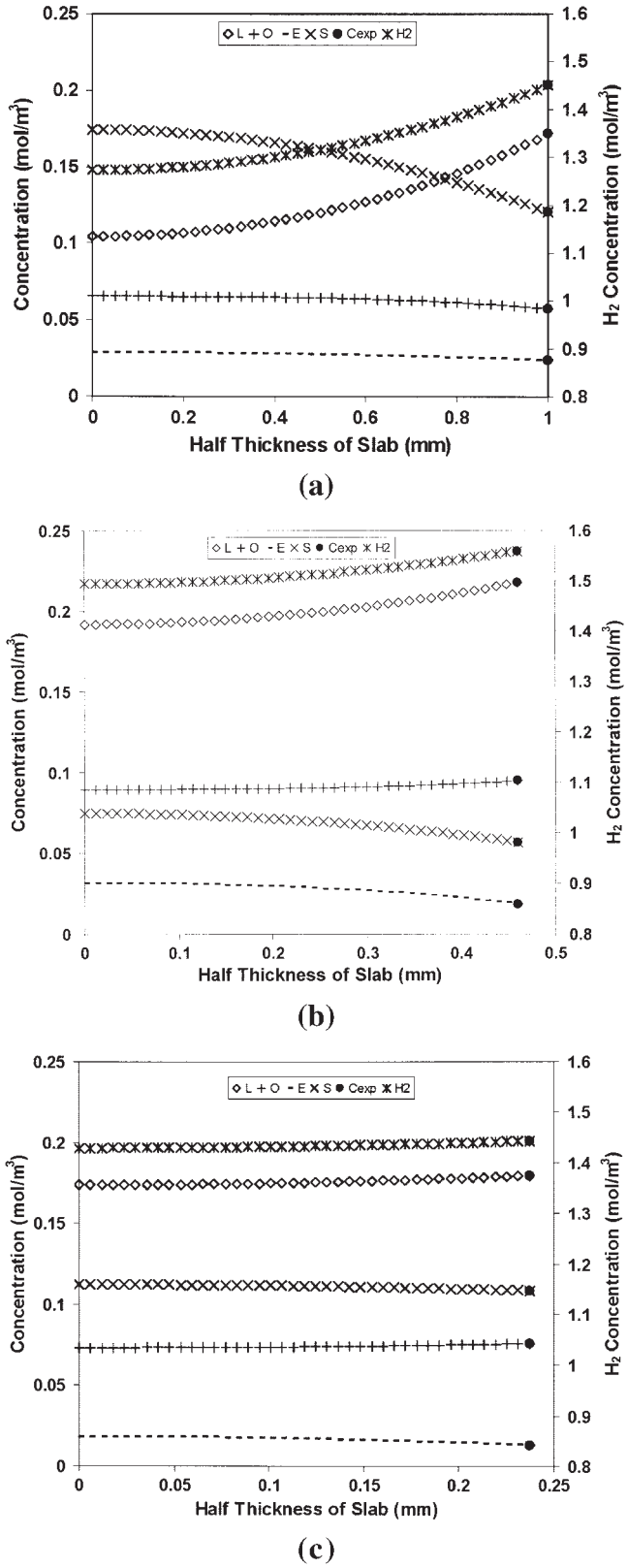

Figure 4. (a) Concentration profiles of hydrogen and sunflower oil components in 2% Pd/C at 484 K, 20 MPa; mol feed composition (oil:H_2:propane): 1:4:95%: (a) d_p = 2 mm; (b) d_p = 0.92 mm; (c) d_p = 0.47 mm.

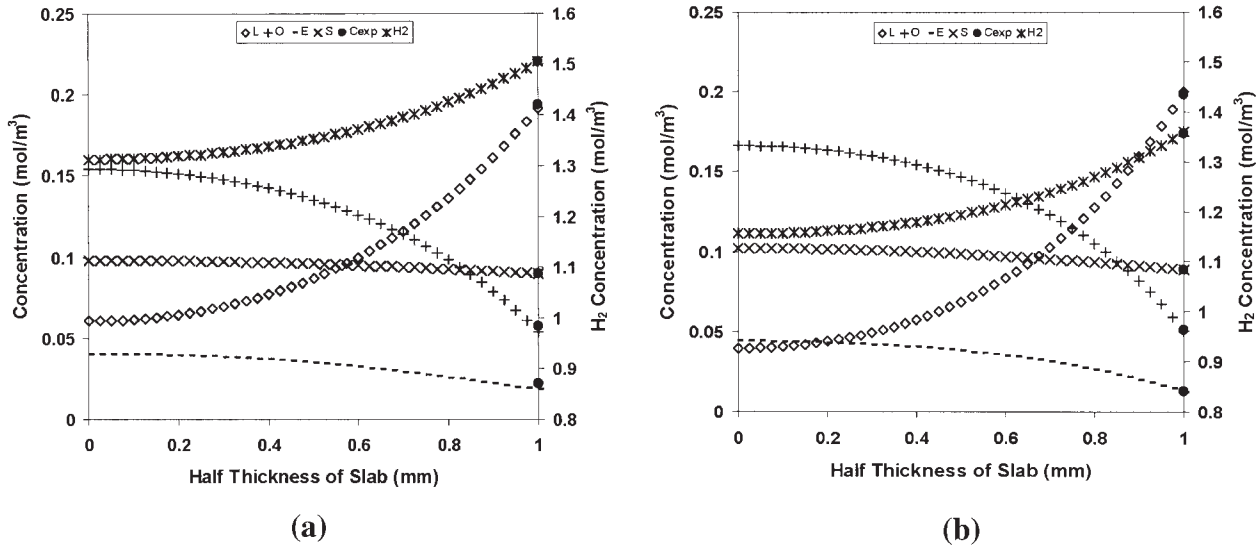

Figure 5. Intraparticle concentration profiles in hydrogenation of sunflower oil in SC propane at 457 K, mol feed composition (oil:H_2:propane): 1:4:95%, and d_p = 2 mm: (a) P = 20 MPa; (b) P = 27.5 MPa.

Results and Discussion

The concentration profiles for each species inside the catalyst particle under different operating conditions are shown in Figures 4, 5, and 6.

For 484 K and 20 MPa, the hydrogen concentration profiles in the larger particles (0.92 and 2 mm) are steeper than those in the smallest particle (0.47 mm), as can be seen in Figures 4a and 4b. In the latter case (Figure 4c), the flat concentration profiles of all components suggest that the internal diffusion rates are rapid, so diffusion is not limiting. The same trend of profiles is observed at 457 K and 20 MPa.

The effect of reaction temperature and pressure on the concentration profiles can be seen in Figures 5 and 6. Pressure does not seem to have as appreciable an effect on the concentration profiles (see Figures 5a and 5b, respectively) as that of temperature (Figure 6), which suggests that the adsorption equilibrium constant for hydrogen as well as for sunflower oil is strongly dependent on temperature, as was previously reported by several authors for low-pressure systems,[65-67] although the catalyst particle effectiveness is generally quite sensitive to temperature in view of the relative activation energies of the intrinsic reaction and diffusion.[68]

The sensitivity of the steady-state diffusion–reaction to the value of D_{e,H_2} was tested at different particle diameters for the case of 484 K, 20 MPa, and a molar feed composition (oil:H_2:propane) of 1:4:95. Rates on smaller particles (0.1 mm) were extrapolated and were included in the model calculations to confirm that there were not intraparticle diffusional resistances. This was verified later when the sensitivity to the diffusivity values was found to be practically irrelevant for particles > 0.1 mm (see Figure 7), to do sensitivity analysis deviations deter-

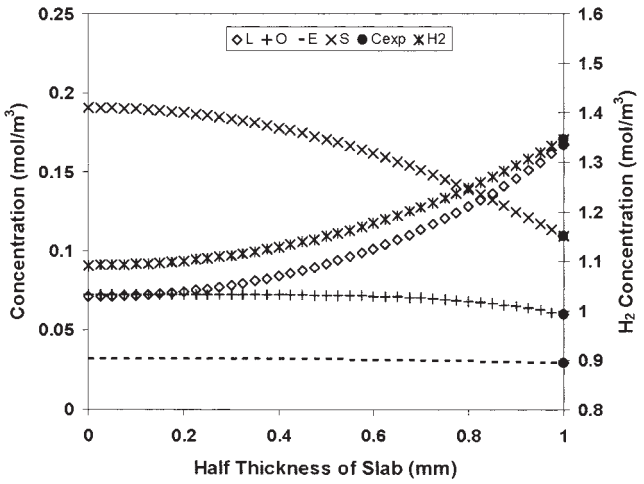

Figure 6. Intraparticle concentration profiles in the catalyst particle in oil hydrogenation in SC propane at 484.15 K, mol feed composition (oil:H_2: propane): 1:4:95%: d_p = 2 mm; P = 27.5 MPa.

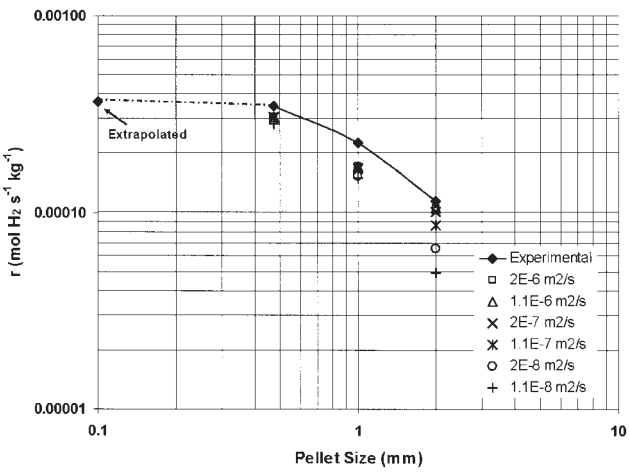

Figure 7. Sensitivity of the proposed model to the values of H_2 effective diffusivity at 484 K, 20 MPa, and a molar feed composition (oil:H_2:C_3H_8) of 1:4: 95%.

Table 5. Model Sensitivity with Fitted Parameters (484 K, 20 MPa, 1:4:95 mol %)

Parameter	Optimized	Test Value	AAD% L = 2 mm	AAD% L = 0.1 mm
k_{12}*	1.56×10^{-4}	1.56×10^{-3}	1.10	5.86
k_{13}*	0.00E+00	1.56×10^{-7}	0.02	0.01
k_{24}**	1.82×10^{-4}	1.82×10^{-3}	3.71	14.50
k_{34}**	3.16×10^{-5}	3.16×10^{-4}	3.92	3.23
k_{23}*	6.66×10^{-4}	6.66×10^{-3}	2.87	87.48
k_{32}*	1.93×10^{-3}	1.93×10^{-2}	4.42	71.60
$D_{e,TG}$†	9.80×10^{-8}	9.80×10^{-7}	69.99	0.006
D_{e,H_2}†	2.00×10^{-7}	2.00×10^{-6}	70.22	0.003

*[mol$^{-1/2}$ (m^3)$^{3/2}$ kg^{-1} s^{-1}].
**[mol^{-1} (m^3)^2 kg^{-1} s^{-1}].
†(m^2 s^{-1}).

mined using the average absolute deviations (AAD%).

Refer to Figure 7, where particles of sizes of 0.4, 0.9, and 2 mm are considered. For the large particles the sensitivity of the model to the diffusivity values was significant because a 10-fold increase or a decrease in the fitted H_2 diffusivity (2×10^{-7} m^2/s) generated a variation on predicted H_2 rates of reaction between 8 and 43%, compared with the experimentally measured values, indicating that this parameter is very sensitive.

The sensitivity of the model to all fitted parameters (intrinsic kinetic constants and effective diffusivities changed by 10-fold or by 1/10-fold) for two particle diameters is presented in Table 5. As seen, at the smallest particle diameter, more accurate values are obtained (less AAD%) for the effective diffusivities than for the kinetic parameters. The situation is the opposite for the largest particle catalyst, as one would expect, thus investing further confidence in the decoupling procedure used based on the relative sensitivities of the model to the values of parameters.

Figure 8 shows the effectiveness factor for several particle diameters. It can be observed that as the particle diameter becomes very small (0.1 mm), the effectiveness factor approaches unity because reaction is kinetically controlled. On the other hand, when the particle diameter increases, the hydrogenation effectiveness factor η becomes unacceptable (that is, $\eta < 0.3$), so the catalyst is far from being fully used in the process.

Table 6 summarizes the intrinsic kinetic parameters for the supercritical sunflower hydrogenation determined from the solution of the combined diffusion–reaction model for the small particle diameter. The value of k_{13} is not representative because this is much smaller than k_{12} (about 5% of it, $k_{13} = 10^{-7}$). This is attributed to the parameter-fitting procedure because the value settled on for the method convergence is 10^{-7}. Special experiments (pure component hydrogenation) are necessary to accurately measure k_{13}.

The minimized χ^2-target function is defined by the following

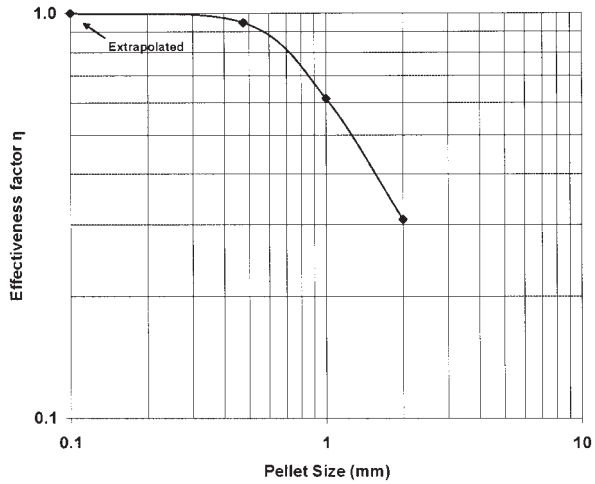

Figure 8. Effectiveness factor for hydrogenation on different catalyst particle sizes (slab geometry).

equation as the square deviation between experimental and predicted model rate of reaction for the hydrogenation species N_q:

$$\chi^2 = \sum_{i=1}^{N_q} \frac{(r_i^{\exp} - r_i^{\text{model}})^2}{r_i^{\text{model}}} \qquad i = \text{L, O, E, S, H}_2 \qquad (13)$$

Thus any possible weighting factors are already taken into account in the chi-squared definition. Other objective functions, based on other probability laws, can be used.[28] The kinetic parameters are obtained by the Levenberg–Marquardt algorithm. The values of $k_{i,j}$ are in the range of 10^{-3}–10^{-6}, and are thus very widely separated. In the Levenberg–Marquardt algorithm, constraints are the inequalities given in Table 7.

As indicated, the fitted kinetic constants were used in the steady-state diffusion and chemical reaction model to obtain the effective diffusivities of oil and H_2, respectively. The estimated diffusivity values under different reaction conditions are summarized in Table 8.

The effective diffusivities results confirm that hydrogen diffuses much more readily (10-fold faster) than the triglycerides. This is the expected behavior based on molecular size. Again, this finding invests confidence in our method.

Second, it is also seen that the increase in temperature or the decrease of system pressure leads to an increase in the effective diffusion coefficients. However, the effect of temperature on diffusivity seems to be more significant than the effect of pressure. This effect of pressure was described by Arunajatesan et al.[6] as a pressure-tunable diffusivity. The increment in effective diffusion coefficients with temperature follows the

Table 6. Intrinsic Kinetic Constants for Sunflower Oil Hydrogenation in SC Propane on Pd/C

T	Kinetic Constants					
(K)	k_{12}*	k_{13}*	k_{24}**	k_{34}**	k_{23}*	k_{32}*
457	1.308×10^{-4}	0.000	3.200×10^{-6}	3.2854×10^{-6}	3.913×10^{-4}	1.456×10^{-3}
484	1.563×10^{-4}	0.000	1.823×10^{-4}	3.161×10^{-5}	6.660×10^{-4}	1.928×10^{-3}

*[mol$^{-1/2}$ (m^3)$^{3/2}$ kg^{-1} s^{-1}].
**[mol^{-1} (m^3)^2 kg^{-1} s^{-1}].

Table 7. Constraints on the Calculated CSTR Concentrations Used on the Levenberg–Marquardt Optimum Search

	CSTR Concentration				
	C_L	C_O	C_E	C_S	C_H
Constraints	$<C_{L0}$	$>1 \times 10^{-5}$	$>1 \times 10^{-5}$	$>C_{S0}$	$<C_{H0}$

trend suggested by Satterfield,[22] who considered that it is "only" proportional to T^n, with n between 1.5 and 2 (just like a molecular diffusion coefficient). In our case the exponent n is around 21, whereas the increment of effective diffusivities with decreasing pressure is directly proportional to P. The trend suggests that the pronounced temperature dependency may arise from the strong effect of temperature on the adsorption equilibrium constants, as we will see later on. The less significant influence of system pressure on the effective diffusivities at higher pressures, in the supercritical region above the critical point of the mixture, is in agreement with the results reported by Arunajatesan et al.[6] and by Suárez et al.[53] for molecular diffusivity in SCF. It is clear, in any case, that the effective diffusivities for triglycerides and hydrogen in the liquid-filled pores (as in the conventional slurry reactor hydrogenation) are much lower than those in the supercritical fluid. Clearly, this is one of the reasons that hydrogenation rates in SCFs are at least 10-fold higher than those in conventional slurry process.[13,14]

The effective diffusivity values for triglycerides agree well with those expected for mixtures of a supercritical gas and a low volatile component (10^{-8} m^2/s), as suggested by Brunner.[63] They are about one order of magnitude higher than those for liquids and about two orders of magnitude lower than those for gases. In the case of hydrogen dissolved in a SC propane, it is expected that the effective diffusivity can be one order of magnitude higher than that in liquids (effective diffusivity is around 10^{-8} m^2/s) because, even though a gas phase is present, the wetting of the catalyst particles by the supercritical fluid means that the pores will be essentially filled with fluid, which has a liquidlike density. Therefore diffusive properties should resemble those in liquid-filled pores.

Selectivities in fat oil hydrogenation in SC propane

From the concentration profiles in the catalyst pellet, the overall reaction rates can be calculated. Then the overall linoleate selectivity (S_{LO}) of the catalyst is defined here as the ratio of the net rate of formation of *cis*-monounsaturated compound to the net rate of formation of saturated species. Under partial diffusional resistance, the linoleate selectivity will be

$$\textit{Linoleate Selectivity } (S_{LO}) = \left. \frac{-\left(\frac{dC_O}{dx}\right)}{-\left(\frac{dC_S}{dx}\right)} \right|_{x=L/2} \tag{14}$$

The value of S_{LO} was determined from the diffusion rates for 484 K, 20 MPa, and molar feed composition (oil:H_2:propane) of 1:4:95 for both the smallest and the largest particles, and these values were compared to those from the definition of selectivity based on the kinetic constants. Following the reaction network of hydrogenation reactions proposed by Elbid and Albright,[69] the linoleate selectivity was then defined as

$$S_{LO} = \frac{k_{12} + k_{32}}{k_{24} + k_{34}} \tag{15}$$

which was valid only in the chemical regime (see Figure 1) and under pseudo-first-order conditions for the oils. In our case, because oil concentrations are very small and can be varied independently, the corresponding expression is

$$S_{LO} = \frac{k_{12}C_L + k_{32}C_E}{k_{24}C_O + k_{34}C_E} \tag{16}$$

At the same time, the specific isomerization (S_i) was considered. This is defined as the ratio of the rate of formation of *trans*-monounsaturated compound to the net rate of hydrogen uptake (see Eq. 17). This was determined from the model and compared with the values from the definition suggested by Coenen.[44] This is defined as the ratio of the percentage increase in *trans*-isomer content and the decrease in iodine value (IV). Expressed in terms of the fluxes, this will be

$$\text{Specific isomerization } (S_i) = \frac{D_{e,TG}}{D_{e,H_2}} \left. \frac{-\left(\frac{dC_E}{dx}\right)}{-\left(\frac{dC_{H_2}}{dx}\right)} \right|_{x=L/2} \tag{17}$$

Table 8. Measured Effective Diffusion Coefficients for Triglycerides and H_2 on 2% Pd/C Catalyst*

T (K)	P (MPa)	$D_{e,TG}$ (m^2 s^{-1} × 10^8)	D_{e,H_2} (m^2 s^{-1} × 10^7)
457	20.0	2.94	0.64
457	27.5	1.72	0.44
484	20.0	9.80	2.00
484	27.5	6.25	1.30

*d_p range = 0.47–2 mm.

The values for S_{LO} and *trans*-selectivity calculated from the fluxes are summarized in Table 9. As can be seen in this table, in the case of the small catalyst particle, the S_{LO} value obtained from Eq. 14 is rather close to that obtained from Eq. 16 because the reaction is kinetically controlled. When the particle diameter is large, however, the diffusion usually limits the overall rate of reaction and, for this reason, the S_{LO} values do not agree.

The selectivity results are in agreement with those reported for low pressure by Tsuto et al.,[46] Coenen,[44] Westerterp et al.,[70] Colen et al.,[45] and Veldsink et al.,[41] who found that in the

Table 9. Estimated Selectivities for SC Sunflower Oil Hydrogenation on 2% Pd/C under 487.15 K, 200 MPa, and Molar Feed Composition (Oil:H_2:Propane) of 1:4:95

Particle Size	Linoleate Selectivity (S_{LO})		Specific Isomerization (S_i)	
(mm)	Eq. 14	Eq. 16	Eq. 17	Coenen[44] Definition
0.1	7.82	6.19	0.05	0.04
2	2.11	6.19	0.08	0.02

hydrogenation of edible oils on porous catalysts, intraparticle mass-transfer limitations not only limit catalyst effectiveness but also change the product selectivities.[61]

Intraparticle mass-transfer mechanisms in SCF

Having measured the kinetic parameters and the diffusion rates within the catalyst, we next look at the possible intraparticle mass-transfer mechanisms for the species involved in the reactions. We base the analysis on the abnormal tortuosity factor (or abnormal values of the ratio D_e/D) observed in a supercritical fluid solvent. Because particle void fractions were not precisely measured, there will be less error using D_e/D. Lai and Tan[36] used this ratio.

To determine the ratio D_e/D, which is related with the tortuosity factor by Eq. 1, the binary molecular diffusivities for oil and H_2 in SC propane were estimated. In the case of triglycerides, we used the Catchpole and King[60] as well as the Sun–Chen[59] correlations in near-critical fluids.

Table 10 presents the estimated molecular diffusivity coefficients for C_3H_8–triglycerides and C_3H_8–H_2 pairs found by means the correlations explained above.

As expected, the molecular diffusivity coefficients for C_3H_8–triglycerides and C_3H_8–H_2 pairs increase with temperature at constant pressure. The rise is proportional to T^m, where m is around 2 for C_3H_8–H_2 and 3 for C_3H_8–triglycerides pair and may arise from the decrease in the solvent density associated with the increase in system pressure.[4]

The molecular diffusivity coefficients are inversely proportional to the molar volume of the solute. As can be seen in Table 10, the triglycerides seem to diffuse at a slower rate than hydrogen in SC propane under comparable experimental conditions.

The general trend observed is that at constant temperature the molecular diffusivities decrease with increasing pressure. It was found that the molecular diffusivities are inversely proportional to total pressure ($D_{12} \propto P^{-1}$). The influence of pressure is essentially the combination of changes in the fluid density and viscosity. As the density of the fluid increases, the molar volume decreases. In such a situation, collision transfer—rather than molecular transfer—becomes the dominant

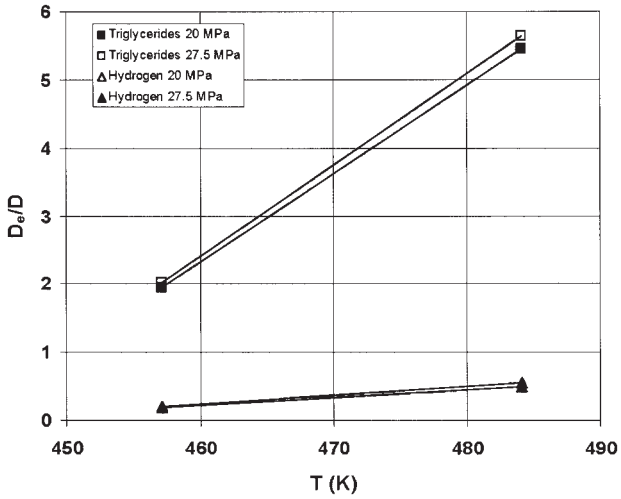

Figure 9. Influence of temperature on the measured ratio (D_e/D) for hydrogen and triglycerides at constant pressure.

transport mechanism, resulting in a more erratic path taken by the solute molecule and consequently in a sharp decrease in diffusivity. This suggests an inverse relationship between diffusion coefficient and solvent density, as shown in Figure 9.

By using the estimated molecular diffusivity values for C_3H_8–triglycerides and C_3H_8–H_2 pairs (Table 10, Figure 10) we determined the ratio of the molecular diffusivity to the effective diffusivity under several operating conditions with the fitted effective diffusivities obtained experimentally. The estimated values are shown in Table 11.

As can be seen from Table 12, hydrogen behaves in the expected way. That is, the ratio $(D_e/D)_{H_2}$ is less than unity, which suggests that for the case of hydrogen, bulk pore diffusion contributes to the mass transport rate. This is a logical consequence because hydrogen can diffuse much more freely than the triglycerides as a result of its smaller molecular size. The average values of $(D_e/D)_{H_2}$ (between 0.07 and 0.14) obtained from Table 1 for several hydrogenations at 6.5 MPa over a wide range of temperatures[22,62] are quite similar to those reported in this study.

In contrast, for triglycerides Table 12 and Figure 9 show a strong effect of temperature on the ratio (D_e/D), whereas the effect of pressure is smaller (Figure 8, see D_e/D at constant T) but still significant. This is a consequence of the strong influence of temperature on the effective diffusion coefficients, presented earlier. It certainly deserves comment.

Considering the random-pore model[31] for a pellet containing micropores, the D_e/D ratio would be equal to the square of the

Table 10. Molecular Diffusivities for C_3H_8–Triglycerides and C_3H_8–H_2 under Several Operating Conditions

Temperature	Pressure	$\rho_{C_3H_8}$	Estimated Binary Diffusion Coefficient D_{12} (m^2/s)		
			C_3H_8–Triglycerides $\times 10^8$		C_3H_8–H_2 $\times 10^7$
(K)	(MPa)	(kg/m^3)	Catchpole and King[60]	Sun and Chen[59]	Satterfield[22]
457	20.0	377	1.62	1.51	3.21
457	27.5	448	0.83	0.85	2.34
484	20.0	300	1.92	1.80	3.58
484	27.5	408	1.25	1.11	2.61

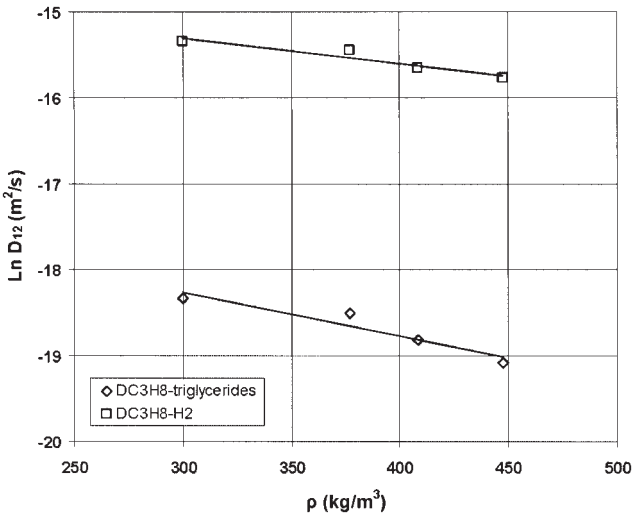

Figure 10. Estimated molecular diffusivity of hydrogen and triglycerides in SC C_3H_8.

catalyst porosity, ε_p^2 (first term in Eq. 2). In the case of 2% Pd/C catalyst whose pore volume consists predominantly of micropores and whose porosity is about 0.45, the $(D_e/D)_{H_2}$ ratio would be 0.25. The results for hydrogen in Table 9 are in a good agreement with this value.

Using the Wakao–Smith theory, $\tau = 1/\varepsilon_p$. In our case, the estimated value of τ is around 2, which is acceptable as a "normal" tortuosity value because tortuosity factors usually range between 2 and 6, averaging about 4, so surface diffusion would not be so significant.[22,28,61]

However, for the case of triglycerides, the D_e/D ratio lay between 1.95 and 5.63, which is considerably too high for bulk diffusivity alone (the ratio D_e/D generally ranges between 0.083 and 0.25[61]). Such high values of $(D_e/D)_{TG}$ (or $\tau < 1$) would mean that triglycerides would diffuse faster between two points through the net of random pores than in a straight line joining the two points: this is clearly impossible! So, to explain these results we postulate that a parallel path for diffusion should be available to the reactants. A potential candidate—an alternative parallel diffusion mechanism—is surface diffusion. If a molecule can diffuse in the bulk fluid of the pore and on the surface, the superposition of these two mechanisms would significantly enhance the transport. Therefore, surface diffusion plays an important role in the intraparticle transport mechanism in diffusion of heavy solutes under reacting conditions.

A prerequisite for surface migration is a strong adsorption of the solute on the pore walls.[35] The trend observed suggests that the triglycerides are preferably absorbed in the pore's wall and then scout along the wall at a faster rate as they move in the bulk. A similar abnormal D_e/D ratio was observed by Lai and Tan[36] for toluene in SC CO_2 in activated carbon pellets under nonreacting conditions.

Equation 2 reflects the cooperation of the two diffusion mechanisms. The estimation of the importance of surface diffusion to pore volume diffusion under several operating conditions is given by the ratio obtained from Eq. 2, dividing both sides by D (results are presented in Table 11).

With some values for the surface diffusion coefficients for triglycerides, it is possible to correlate these values with the usual estimation methods of surface diffusion. Sladek et al.[39] proposed a correlation for the diffusivities of physically and chemically adsorbed species directly related to the heat of adsorption ($-\Delta H$). The D_s values for triglycerides on activated carbon are determined from this correlation using the previously estimated heat of adsorption. Figure 12 presents the Sladek correlation with several experimental points along with the predicted values of this study. The original Sladek correlation has been extended to positive ΔH values to cover our data points; as seen the correlation is still useful. We mention here that positive enthalpy change values are possible in SC fluids, as shown by the modeling of the retrograde effects.[37,58,71] Even far above the critical point, but below the crossover pressure, retrograde adsorption equilibrium is still possible. In this region, it involves a reversed type of linear isotherm.

Table 11. D_e/D Ratio for Triglycerides and Hydrogen in SC Propane for Different Reaction Conditions on 2% Pd/C

Reaction Temperature (K)	Pressure (MPa)	$(D_e/D)_{TG}$	$(D_e/D)_{H_2}$
457	20.0	1.95	0.20
457	27.5	2.03	0.19
484	20.0	5.44	0.56
484	27.5	5.63	0.50

The magnitude of D_s estimates (1.58×10^{-5} and 1.26×10^{-5} m^2/s at 457 and 484 K, respectively) are quite similar to those characteristic of physical adsorption systems, which typically range from 10^{-9} to 10^{-6} m^2/s and are considerably higher than those reported for surface diffusion in chemisorption systems.[39] From these results and taking into account the ratio $(\rho_p K_A D_s)/D$ (see Figure 12 and Table 12), the importance of surface diffusion of triglycerides is likely attributable to the value of K_A rather than to the value of D_s itself because the latter is a weak function of temperature, as reported in the literature. Therefore, the triglyceride molecules may exhibit a high mobility associated with their low energies of physical bonding onto the pore wall in comparison with that typical of chemically adsorbed molecules.

Another phenomenon that could be present in the case of triglycerides is restricted diffusion. This occurs when the dimensions of the solute molecule ($1.5–2 \times 10^{-6}$ mm for triglycerides) and the pore ($2–3 \times 10^{-6}$ mm for 2% Pd/C catalyst) are comparable. In this case, a hindered diffusion factor ($\sim$0.7) has to be taken into account, which depends on the diameter ratio of molecule and pore, d_s/d_e. Using Eq. 1, it is possible to make a rough estimate of the tortuosity factor. The values thus obtained are much less than unity, and thus they confirm the significance of the surface diffusion hypothesis.

Table 12. Values of the Group $(\rho_p K_A D_s)/D$ for Triglycerides in SC Propane under Reaction Conditions on 2% Pd/C Catalyst

Temperature (K)	Pressure (MPa)	$(\rho_p K_A D_s)/D$
457	20.0	3.88
457	27.5	4.05
484	20.0	11.65
484	27.5	12.06

Conclusions

The diffusive properties of different species in a Pd catalyst have been studied for the hydrogenation of sunflower oil using propane as a supercritical solvent. A single vapor-phase continuous process was operated using an internal recycle, Robinson–Mahoney catalytic reactor.[72] The effective diffusivity of hydrogen and triglyceride components within the porous catalyst have been measured using reaction experiments. To our knowledge, a study on the mechanism of diffusion and measurements of the diffusivities on a catalyst matrix (activated carbon) filled with dense gas was unavailable to date. Data from extraction (or straight mass transfer) with SCF, under nonreacting conditions, were previously published.[23] Comparison with the present results show that diffusion in the pore network, either in the presence or absence of reaction, is abnormal, given that the ratio $D_e/D \gg 1$.

The method of measuring the effective diffusion coefficients was first to obtain the intrinsic kinetic constants on small-size catalyst particles (0.5 mm) in the absence of diffusional limitation. Then, using the intrinsic kinetic constants we could derive the diffusivities in diffusion-limited reaction runs.

In a way, the system studied partly confirms the findings of a nonreacting system. That is, the ratio of D_e/D is >1 for triglycerides. This is in agreement with the mass transfer without reaction of Knaff and Schlünder,[57] Lai and Tan,[36] and others. For hydrogen, however, diffusion properties and tortuosity factors are completely normal. This is interpreted in terms of surface diffusion for the heavier oil components that tend to be adsorbed/desorbed to the pore walls and thus diffuse along them in a parallel path to bulk pore diffusion. This is not surprising in view of the more compact structure of the dense fluid that rejects the higher molecular weight solutes to the wall.

By varying pressure and then temperature, we could measure the variation of surface diffusion with P and T. The effect of the surface diffusivity with pressure completely agrees with the findings of Subramaniam and coworkers,[6] so a pressure-tuning effect was also observed. The largest effect, however, is a strong impact of temperature on surface diffusion. This large effect suggests that adsorption of oil on the pore walls controls diffusion, so that surface migration is a key mechanism for diffusion in pores filled in a supercritical fluid, at least for solutes that are relatively heavier (MW $>$ 500)

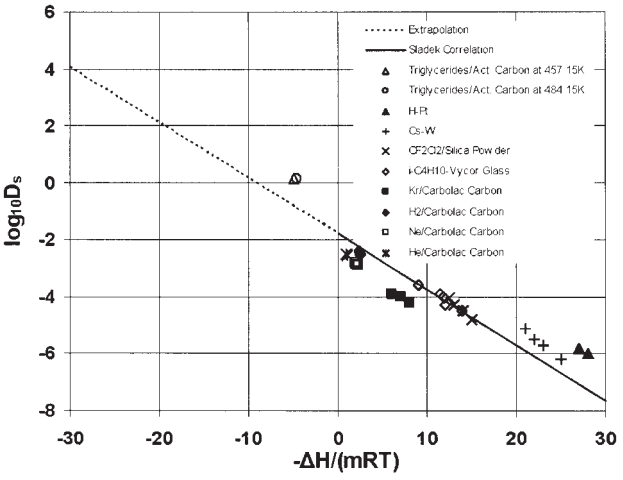

Figure 11. Prediction of surface diffusivities by the Sladek et al.[39] correlation (with m = 1–3), extended to the positive values of ΔH.

Triglyceride data, four upper points, as measured in this study.

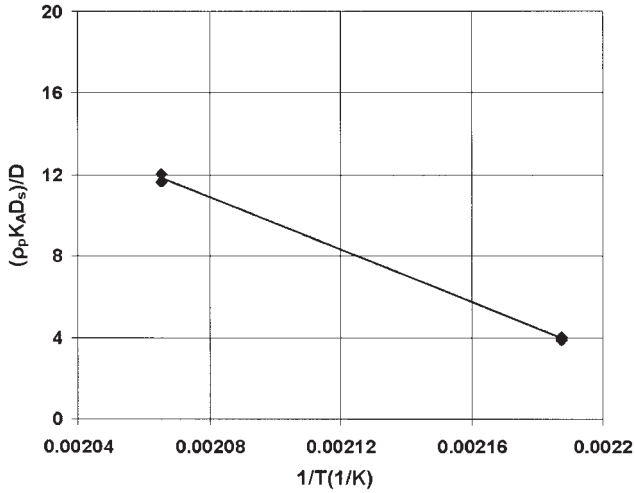

Figure 12. Variation of the surface diffusion contribution group $(\rho_p K_A D_s)/D$ with temperature for two pressures.

The values of linoleic selectivities and stearic yield were calculated using the diffusion flux equations for the cases where diffusion controlled the rate of hydrogenation. For large particles, of course, the values calculated with kinetic constants differ from the true ones only because of the presence of diffusion gradients. Reaction is very fast in the Pd particles: the effectiveness factor for overall hydrogenation for a catalyst size of 1 mm is 0.7 and for 2 mm the effectiveness is only 0.3. This opens up the question as to which reactor/catalyst should be used industrially to take advantage of the full reaction rate and potential selectivities.

The Sladek et al.[39] correlation was used to make a regression of a few data points on the surface diffusivity D_s generated in the present study. We found that they could be well predicted by the Sladek straight line, provided that it is extended to positive values of the enthalpy of adsorption, considered for estimating surface diffusion coefficients. This is most interesting because the heat of adsorption may be estimated from high-pressure, phase equilibrium thermodynamics, and then by use of the Sladek correlation, which requires a value for ΔH, to obtain D_s. Alternatively, the Henry adsorption equilibrium constant and heat of adsorption can be determined by supercritical chromatography[71] in a rather simple way.

Acknowledgments

E. Ramírez Rangel received a predoctoral fellowship from AGAUR (Generalitat de Catalunya, Spain). The financial support of the Spanish Ministry of Education and Science (Grant number of joint CICYT-FEDER AGL 2003-05861, Madrid and Brussels) is gratefully acknowledged.

Notation

C_i = mol concentration, mol/m^3, i = L, O, E, S, H_2
C_{i_s} = concentration of i at catalyst surface, mol/m^3, i = L, O, E, S, H_2

d_p = spherical diameter of particle, m
d_s = solute molecule diameter, m
d_e = pore diameter, m
D = molecular diffusion coefficient, m^2/s
D_{12} = binary diffusion coefficient, m^2/s
D_e = effective diffusivity, m^2/s; effective diffusivity of triglycerides = $D_{e,TG}$, effective diffusivity of hydrogen = D_{e,H_2}
D_s = surface diffusion coefficient, m^2/s
E = activation energy, J/mol K; E_S = for surface diffusion, E_D = for molecular diffusion
IV = iodine value, g I_2/100 g oil
K_A = adsorption equilibrium constant on the solid from the high-pressure fluid
k_{ij} = kinetic constants in the network of Figure 1 based on a kg cat (see units in Tables 5 and 6)
L = slab thickness, m
m = coefficient in Sladek correlation
$r_{p,i}$ = reaction rate of formation per pellet mass, mol i/(kg s)
R = ideal gas-law constant, J/(mol K)
S_{LO} = linoleate selectivity; see Eq. 14
S_i = specific isomerization yield; see Eq. 15
T = temperature, K
ΔH = enthalpy change on adsorption, J/(mol K)
x = coordinate perpendicular to slab, m
z_i, = concentration gradient = dC_i/dx, mol/m^4

Greek letters

ε_p = pellet void fraction
ρ_p = pellet density, kg/m^3
χ^2 = chi-squared; see Eq. 13
τ = tortuosity factor

Acronyms

AAD = average absolute deviation
E = elaidic fatty acid, *trans* C18:1
FAME = fatty acid methyl ester
H_2 = hydrogen
L = linoleic fatty acid, C18:2
O = oleic fatty acid, *cis* C18:1
ODE = ordinary differential equation
S = stearic fatty acid, C18:0
SC = supercritical
SCF = supercritical fluid
TAG = triacylglycerol
TG = triglyceride
C_3H_8 = propane

Literature Cited

1. King JW, List GR. *Supercritical Fluid Technology in Oil and Lipid Chemistry.* Champaign, IL: The American Oil Chemists' Society; 1996.
2. Brunner G. *Supercritical Fluids as Solvents and Reaction Media.* Amsterdam, The Netherlands: Elsevier; 2003.
3. Ajzenberg N, Trabelsi F, Recasens F. What's new in industrial polymerization with supercritical solvents? *Chem Eng Technol.* 2000;23: 829-839.
4. Subramaniam B, McHugh M. Reactions in supercritical fluids—A review. *Ind Eng Chem Res.* 1985;25:1-30.
5. Baptist-Nguyen S, Subramaniam B. Coking and activity of porous catalysts in supercritical reaction media. *AIChE J.* 1992;38:1027-1037.
6. Arunajatesan V, Wilson KA, Subramaniam B. Pressure tuning the effective diffusivity of near-critical reaction mixtures in mesoporous catalysts. *Ind Eng Chem Res.* 2003;42:2639-2643.
7. Wisniak J, Albright LF. Hydrogenating cottonseed oil at relatively high pressure. *Ind Eng Chem.* 1961;53:375-380.
8. Farrauto RJ, Bartholomew CH. *Fundamentals of Industrial Catalytic Processes.* London, UK: Chapman & Hall; 1997.
9. Rase HF. *Handbook of Commercial Catalysts: Heterogeneous Catalysts.* Boca Raton, FL: CRC Press; 2000.
10. Rase HF. *Chemical Reactor Design for Process Plants, Vol. II: Case Studies and Design Data*. New York, NY: Wiley; 1977.
11. Horiuti J, Polanyi M. Exchange reactions of hydrogen on metallic catalysts. *Trans Faraday Soc.* 1934;30:1164-1172.
12. King JW, Holliday RL, List GR, Snyder JM. Hydrogenation of vegetable oils using mixtures of supercritical carbon dioxide and hydrogen. *J Am Oil Chem Soc.* 2001;78:107-114.
13. Härrod M, Van den Hark S, Macher MB, Moller P. Hydrogenation at supercritical single-phase conditions. In: Bertucco A, Vetter G, eds. *High Pressure Process Technology: Fundamentals and Applications.* New York, NY: Elsevier; 2001.
14. Ramírez E, Zgarni S, Larrayoz MA, Recasens F. Short compilation of published rate data for catalytic hydrogenations in supercritical fluids. *Chem Eng Technol: Eng Life Sci.* 2002;2:257-264.
15. Härröd M, Møller P. Hydrogenation of fats and oils at supercritical conditions. In: Rudolf von Rohr P, Trepp Ch, eds. *Proceedings of the 3rd International Symposium on High-Pressure Chemical Engineering.* Zurich, Switzerland: Elsevier; 1996:43-48.
16. Tacke T, Wieland S, Panster P. Hardening of fats and oils. In: Rudolf von Rohr P, Trepp Ch, eds. *Proceedings of the 3rd International Symposium on High-Pressure Chemical Engineering.* Zurich, Switzerland: Elsevier; 1996:17-22.
17. Tacke T, Wieland S, Panster P. Selective and complete hydrogenation of vegetable oils and free fatty acids in supercritical fluids. In: De Simone JM, ed. *Green Chemistry Using Liquid and Supercritical Carbon Dioxide*. Oxford, UK: Oxford Univ. Press; 2003.
18. Box G, Draper NR. *Empirical Model-Building and Response Surfaces*. New York, NY: Wiley; 1987.
19. Ramírez E, Recasens F, Fernández M, Larrayoz MA. Hydrogenation of sunflower oil on Pd/C in supercritical propane: Operating conditions in a continuous internal recycle reactor. *AIChE J.* 2004;50:1545-1555.
20. Hashimoto K, Muroyama K, Nagata S. Kinetics of the hydrogenation of fatty oils. *J Am Oil Chem Soc.* 1971;48:291-295.
21. Camps S, Fernández M, Larrayoz MA, Ramírez E, Recasens F, Sans J. Proceso de hidrogenación parcial de triglicéridos insaturados en fase vapor a alta presión y reactor para la realización de dicho proceso. Spain Patent Application P200401793; 2004.
22. Satterfield CN. *Mass Transfer in Heterogeneous Catalysis*. Cambridge, MA: MIT Press; 1970.
23. Stüber F, Julien S, Recasens F. Internal mass transfer in sintered metallic pellets filled with supercritical fluid. *Chem Eng Sci.* 1997;52: 3527-3542.
24. Satterfield CN, Katzer JR. The counterdiffusion of liquid hydrocarbons in type Y zeolites. *Adv Chem Ser.* 1971;102:193-200.
25. Satterfield CN, Cheng CS. Liquid counter diffusion of selected aromatic and naphthenic hydrocarbons in type Y zeolites. *AIChE J.* 1972;18:724-728.
26. Moore RM, Katzer JR. Counterdiffusion of liquid hydrocarbons in type Y zeolites. Effect of molecular size, molecular type, and direction of diffusion. *AIChE J.* 1982;18:816-824.
27. Satterfield CN, Colton CK, Pitcher WH. Restricted diffusion in liquids within fine pores. *AIChE J.* 1973;19:628-635.
28. Froment GF, Bischoff KB. *Chemical Reactor Analysis and Design.* 2nd Edition. New York, NY: Wiley; 1990.
29. Cussler E. *Diffusion: Mass Transfer in Fluid Systems.* Cambridge, UK: Cambridge Univ. Press; 1997.
30. Wheeler A. Reaction rates and selectivity in catalyst pores. *Adv Catal.* 1952;3:323-328.
31. Wakao N, Smith J. Diffusion in catalyst pellets. *Ind Eng Chem Fundam Q.* 1964;3:123-127.
32. Johnson MFL, Stewart WE. Pore structure and gaseous diffusion in solid catalysts. *J Catal.* 1965;4:248-253.
33. Patel PV, Butt JB. Multicomponent diffusion in porous catalysts. *Ind Eng Chem Proc Des Dev.* 1974;14:298-304.
34. Zalc JM, Reyes SC, Iglesia E. The effects of diffusion mechanism and void structure on transport rates and tortuosity factors in complex porous structures. *Chem Eng Sci.* 2004;59:2947-2960.
35. Koriyama H, Smith JM. Intraparticle mass transport in liquid-filled pores. *AIChE J.* 1974;20:728-734.
36. Lai C, Tan C. Measurements of effective diffusivities of toluene in activated carbon in the presence of supercritical carbon dioxide. *Ind Eng Chem Res.* 1993;32:1717-1722.
37. Recasens F, Velo E, Larrayoz MA, Puigggené J. Endothermic char-

acter of toluene adsorption from SC carbon dioxide onto activated carbon at low coverage. *Fluid Phase Equilib.* 1993;90:265-287.
38. Dedrick RL, Beckman RB. Diffusion in porous particles. *Chem Eng Prog Symp Ser.* 1967;74:63-72.
39. Sladek KJ, Gilliland ER, Baddour RF. Diffusion on surfaces. II. Correlation of diffusivities of physically and chemically adsorbed species. *Ind Chem Fundam.* 1974;13:100-105.
40. Schneider P, Smith JM. Chromatographic study of surface diffusion. *AIChE J.* 1968;14:886-895.
41. Veldsink JW, Bouma MJ, Schöön NH. Beenackers AACM. Heterogeneous hydrogenation of vegetable oils: A literature review. *Catal Rev Sci Eng.* 1997;39:253-318.
42. Bern L, Hell M, Schöön NH. Kinetics of hydrogenation of rapeseed oil: I. Influence of transport steps in kinetic study. *J Am Oil Chem Soc.* 1975;52:182-187.
43. Cordova WA, Harriot P. Mass transfer resistances in the palladium-catalyzed hydrogenation of methyl linolelate. *Chem Eng Sci.* 1975;30: 1201-1206.
44. Coenen JWE. Catalytic hydrogenation of fatty oils. *Ind Eng Chem Fundam.* 1986;25:43-52.
45. Colen GCM, Van Duijn G, Van Oosten HJ. Effect of pore diffusion on the triacylglycerol distribution of partially hydrogenated trioleoylglycerol. *Appl Catal.* 1988;43:339-350.
46. Tsuto K, Harriott P, Bischoff KB. Intraparticle mass transfer effects and selectivity in the palladium-catalyzed hydrogenation of methyl linoleate. *Ind Eng Chem Fundam.* 1978;17:199-205.
47. Andersson K, Hell M, Löwendahl L, Shöön NH. Diffusivities of hydrogen and glyceryl trioleate: I. Cottonseed oil at elevated temperature. *J Am Oil Chem Soc.* 1974;51:171-173.
48. Ganguli KL, van den Berg HJ. Measurements of hydrogen-edible oil interfacial area using a homogeneous Zeigler–Natta catalyst in an agitated reactor. *Chem Eng J.* 1978;16:193-202.
49. Jonker GH, Veldsink JW, Beenackers AACM. Intraparticle diffusion limitations in the hydrogenation of monounsaturated edible oils and their fatty acid methyl esters. *Ind Eng Chem Res.* 1998;37:4646-4656.
50. Veldsink JW. Selective hydrogenation of sunflower seed oil in a three-phase catalytic membrane reactor. *J Am Oil Chem Soc.* 2001;78: 443-449.
51. Liong KK, Wells PA, Foster NR. Diffusion in supercritical fluids. *J Supercrit Fluids.* 1991;4:91-108.
52. Roth TH. Diffusion and thermodynamic measurements by supercritical fluid chromatography. *J Microcol Sep.* 1991;3:173-178.
53. Suárez JJ, Bueno JL, Medina I. Determination of binary diffusion coefficients of benzene and derivates in SC carbon dioxide. *Chem Eng Sci.* 1993;48:2419-2427.
54. Van den Hark S. *The Use of Supercritical Fluids to Reduce the Number of Phases in Catalytic Hydrogenation: The Reaction of Fatty Acid Methyl Esters to Fatty Alcohols.* PhD Thesis. Göteborg, Sweden: Chalmers University of Technology; 2000.
55. Liong KK, Wells PA, Foster NR. Diffusion of fatty acid esters in supercritical carbon dioxide. *Ind Eng Chem Res.* 1992;31:390-399.
56. Lee CH, Holder GD. Use of supercritical chromatography for obtaining mass transfer coefficients in fluid–solid systems at supercritical conditions. *Ind Eng Chem Res.* 1995;34:906-914.
57. Knaff G, Schlünder EU. Mass transfer for dissolving solids in supercritical carbon dioxide, Part I. Resistance of the boundary layer. *Chem Eng Process.* 1987;21:151-160.
58. Recasens F, McCoy BJ, Smith JM. Desorption processes: Supercritical fluid regeneration of activated carbon. *AIChE J.* 1989;35:951-958.
59. Sun CKJ, Cheng SH. Tracer diffusion in dense methanol and 2-propanol up to supercritical region: Understanding of solvent molecular association and development of an empirical correlation. *Ind Eng Chem Res.* 1987;26:815-819.
60. Catchpole OJ, King MB. Measurement and correlation of binary diffusion coefficients in near critical fluids. *Ind Eng Chem Res.* 1994; 33:1828-1837.
61. Smith JM. *Chemical Engineering Kinetics.* 3rd Edition. New York, NY: McGraw-Hill; 1981.
62. Butt JB. *Reaction Kinetics and Reactor Design.* 2nd Edition. New York, NY: Marcel Dekker; 2000.
63. Brunner G. *Gas Extraction—An Introduction to Fundamentals of Supercritical Fluids and the Application to Separation Processes.* Darmstadt, Germany: Steinkopff-Verlag/Springer-Verlag; 1994.
64. Riggs JB. *An Introduction to Numerical Methods for Chemical Engineers.* Lubbock, TX: Texas Tech Univ. Press; 1988.
65. Smeds S, Salmi T, Lindfors LP, Krause O. Chemisorption and TPD studies of hydrogen on Ni/Al_2O_3. *Appl Catal.* 1996;144:177-184.
66. Singh UK, Vannice MA. Liquid-phase hydrogenation of citral over Pt/SiO_2 catalyst. I. Temperature effects on activity and selectivity. *J Catal.* 2000;191:165-172.
67. Rautanen PA, Aittamma JR, Krause AOI. Solvent effect in liquid-phase hydrogenation of toluene. *AIChE J.* 2000;49:1508-1515.
68. Levenspiel O. *Chemical Reaction Engineering.* New York, NY: Wiley; 1999.
69. Elbid IA, Albright LF. Operating variables in hydrogenating cottonseed oil. *Ind Eng Chem.* 1967;49:825-831.
70. Westerterp KR, Van Swaaij WPM, Beenackers AACM. *Chemical Reactor Design and Operation.* New York, NY: Wiley; 1987.
71. Kelley FD, Chimowitz ED. Near-critical phenomena in supercritical fluid chromatography. *AIChE J.* 1990;36:1163-1175.
72. Mahoney JA, Robinson KK, Myers EC. Catalyst evaluation with the gradientless reactor. *Chemtech.* 1978;12:758-763.
73. Madras G, Thibau C, Erkey C, Angerman A. Modeling of supercritical extraction of organics from solid matrices. *AIChE J.* 1994;40:777-785.

Manuscript received Jul. 18, 2005, and revision received Nov. 9, 2005.